OPEN ACCESS
IOP Publishing

Journal of Physics A: Mathematical and Theoretical

J. Phys. A: Math. Theor. **56** (2023) 285302 (12pp)

https://doi.org/10.1088/1751-8121/acdcd1

Helical beams of electrons in a magnetic field: new analytic solutions of the Schrödinger and Dirac equations

Iwo Bialynicki-Birula[1,*] and **Zofia Bialynicka-Birula**[2]

[1] Center for Theoretical Physics, Polish Academy of Sciences Aleja Lotników 32/46, 02-668 Warsaw, Poland
[2] Institute of Physics, Polish Academy of Sciences Aleja Lotników 32/46, 02-668 Warsaw, Poland

E-mail: birula@cft.edu.pl

Received 10 March 2023; revised 11 May 2023
Accepted for publication 8 June 2023
Published 22 June 2023

Abstract

We derive new solutions of the Schrödinger, Klein–Gordon and Dirac equations which describe the motion of particles in a uniform magnetic field. In contrast to the well known stationary solutions, our solutions exhibit the behavior of quantum particles which very closely resembles classical helical trajectories. These solutions also serve as an illustration of the meaning of the Ehrenfest theorem in relativistic quantum mechanics.

Keywords: Dirac equation, motion in magnetic field, Schrödinger equation

(Some figures may appear in colour only in the online journal)

1. Introduction

According to classical mechanics charged particles move in a uniform magnetic field along helical trajectories (figure 1). In this work we describe new solutions of the Schrödinger, the Klein–Gordon and the Dirac equations which are close counterparts of the classical trajectories.

Analytic solutions of wave equations in quantum mechanics are typically obtained by the separation of variables and the time variable is usually the first variable which is subjected to

[*] Author to whom any correspondence should be addressed.

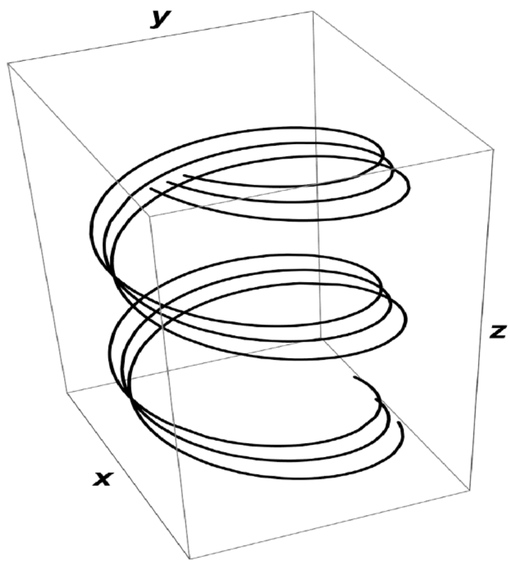

Figure 1. Helical trajectories of classical charged particles in a uniform magnetic field for three choices of initial conditions.

this procedure. This yields the stationary solutions—energy eigenstates. The wave functions obtained in this way do not resemble their classical counterparts because the probability density does not depend on time—nothing moves. For example, the wave functions of stationary states in the Coulomb potential and the elliptical Keplerian orbits do not share any similarities. While it is possible to exhibit the classical-quantum relation by superposing Coulombic wave functions with different orientations of the z axis and with different phases, this task is quite cumbersome and has not yet been accomplished.

Analytic solutions of the Schrödinger and Dirac equations for a charged particle in a uniform magnetic field have been known for almost hundred years [1, 2]. They have been described in detail in [3]. However, these are all stationary solutions, so that the probability density is time-independent. Hence, they cannot be viewed as quantum counterparts of the classical helical trajectories depicted in figure 1.

Our method of constructing new solutions of the Schrödinger and Dirac equations employs the procedure that might be called the injection of classical trajectories (ICT) into the wave functions. This method has been applied to the solutions of the Gross-Pitaevskii equation [4] and to the center of mass motion of Bose–Einstein condensate in a harmonic trap [5]. In the present work we apply this method to the motion of electrons in a magnetic field, both in the nonrelativistic and in the relativistic domain. The states of quantum particles described by the wave functions obtained here are as close as possible to their classical counterparts. The center of the wave packet (defined as the quantum-mechanical average of position) follows the classical trajectory.

2. Classical dynamics

The classical trajectories will be described here within the canonical Hamiltonian formalism because the classical trajectories used in the ICT method are most easily expressed in terms of canonical variables,

$$\boldsymbol{p} = \{p_x, p_y, p_z\}, \quad \boldsymbol{r} = \{x, y, z\}. \tag{1}$$

Moreover, in this formalism the equations of motion have the same form in the nonrelativistic and in the relativistic case.

The starting point are the formulas for the Hamiltonian describing a charged particle in a constant magnetic induction field $\boldsymbol{B}$ in the nonrelativistic and in the relativistic case,

$$H_{\rm NR} = \frac{1}{2m}\left(\boldsymbol{p} - e\boldsymbol{A}\right)^2, \tag{2}$$

$$H_{\rm RL} = c\sqrt{m^2c^2 + \left(\boldsymbol{p} - e\boldsymbol{A}\right)^2}. \tag{3}$$

For the electron e is negative.

We found it convenient to use the geometrical units $1/\text{meter}^2$ for the magnetic induction. This means that in our notation B is related to its counterpart in the SI units by the formula $B = eB_{\rm SI}/\hbar$.

In the case of a constant vector $\boldsymbol{B}$ in the symmetric gauge we have,

$$e\boldsymbol{A} = \frac{\hbar}{2}\boldsymbol{B}\times\boldsymbol{r}. \tag{4}$$

If the z axis is chosen in the direction of $\boldsymbol{B}$, the Hamiltonians (2) and (3) take on the form,

$$H_{\rm NR} = \frac{1}{2m}\left[\boldsymbol{p}^2 + \frac{(\hbar B)^2}{4}(x^2+y^2) - \hbar B(xp_y - yp_x)\right], \tag{5}$$

$$H_{\rm RL} = c\sqrt{m^2c^2 + 2mH_{\rm NR}}. \tag{6}$$

The canonical equations of motion in the nonrelativistic and in the relativistic case have the same form,

$$\frac{dx(t)}{dt} = \frac{p_x(t)}{M} + \frac{\hbar B}{2M}y(t), \tag{7a}$$

$$\frac{dy(t)}{dt} = \frac{p_y(t)}{M} - \frac{\hbar B}{2M}x(t), \tag{7b}$$

$$\frac{dz(t)}{dt} = \frac{p_z(t)}{M}, \tag{7c}$$

$$\frac{dp_x(t)}{dt} = -\frac{(\hbar B)^2 x(t)}{4M} + \frac{\hbar B}{2M}p_y(t), \tag{7d}$$

$$\frac{dp_y(t)}{dt} = -\frac{(\hbar B)^2 y(t)}{4M} - \frac{\hbar B}{2M}p_x(t), \tag{7e}$$

$$\frac{dp_z(t)}{dt} = 0. \tag{7f}$$

The only difference is in the meaning of the parameter M. In the nonrelativistic case, M is simply the rest mass of the particle ($M = m$), while in the relativistic case M denotes the relativistic mass ($M = H_{\rm RL}/c^2$), which is a constant of motion, whose value depends on the initial conditions. The solutions of equations (7) are,

$$x(t) = \frac{1}{2}x_0(1+\cos(\omega t)) + \frac{1}{2}y_0\sin(\omega t) + \frac{p_{x0}\sin(\omega t)}{M\omega} + \frac{p_{y0}(1-\cos(\omega t))}{M\omega}, \tag{8a}$$

$$y(t) = -\frac{1}{2}x_0\sin(\omega t) + \frac{1}{2}y_0(1+\cos(\omega t)) - \frac{p_{x0}(1-\cos(\omega t))}{M\omega} + \frac{p_{y0}\sin(\omega t)}{M\omega}, \tag{8b}$$

$$z(t) = z_0 + \frac{p_{z0}}{M}t, \tag{8c}$$

$$p_x(t) = -\frac{1}{4}x_0 M\omega\sin(\omega t) - \frac{1}{4}y_0 M\omega(1-\cos(\omega t)) + \frac{1}{2}p_{x0}(1+\cos(\omega t)) + \frac{1}{2}p_{y0}\sin(\omega t), \quad (8d)$$

$$p_y(t) = \frac{1}{4}x_0 M\omega(1-\cos(\omega t)) - \frac{1}{4}y_0 m\omega\sin(\omega t) - \frac{1}{2}p_{x0}\sin(\omega t) + \frac{1}{2}p_{y0}(1+\cos(\omega t)), \quad (8e)$$

$$p_z(t) = p_{z0}, \quad (8f)$$

where $\omega = \hbar B/M$ is the cyclotron frequency and the parameters with the subscript 0 denote the initial values of positions and momenta. The trajectories in figure 1 depict these solutions.

3. Helical solutions of the Schrödinger equation

We start with the construction of helical trajectories of the electrons described by the solutions of the Schrödinger equation. In order to treat the motion in a magnetic field, we need an extension of the ICT method used in [4, 5] to cover the case of the Hamiltonian (5) which in addition to the harmonic potential contains also the part with positions and momenta. The extended version of the ICT method can be stated as the following theorem.

Consider the Schrödinger equation with a general quadratic Hamiltonian operator,

$$\hat{H} = \frac{1}{2}\hat{p}_i A^{ij}\hat{p}_j + \frac{1}{2}\hat{x}^i B_{ij}\hat{x}^j + \hat{p}_i C^i{}_j\hat{x}^j. \quad (9)$$

We introduced here upper and lower indices to make use of the Einstein summation convention. The Hamiltonian is obtained from its classical counterpart (2) by replacing the canonical variables with the operators $\hat{x}^i$ and $\hat{p}_i$. In our case the diagonal elements $C^i{}_i$ vanish so that there in no need for the symmetrization of the last term.

The theorem states that from any solution $\psi(x,y,z,t)$ of the Schrödinger equation with the Hamiltonian (9), one can obtain a family of new solutions $\psi_{\mathrm{ICT}}(x,y,z,t)$ defined by the following unitary mapping:

$$\psi_{\mathrm{CT}}(x,y,z,t) = \hat{U}\psi(x,y,z,t) = \exp\left[-\frac{i}{2\hbar}p_i(t)x^i(t)\right]\exp\left[\frac{i}{\hbar}p_i(t)\hat{x}^i\right]\exp\left[-\frac{i}{\hbar}\hat{p}_i x^i(t)\right]\psi(x,y,z,t), \quad (10)$$

where $(x^i(t), p_j(t))$ obey the classical equations of motion,

$$\frac{dx^i(t)}{dt} = A^{ij}p_j(t) + C^i_j x^j(t), \quad (11)$$

$$\frac{dp_i(t)}{dt} = -B_{ij}x^j(t) - C^j{}_i p_j(t). \quad (12)$$

The proof of the theorem (see the appendix) consists in showing that the unitary operator $\hat{U}$ leaves the Schrödinger equation intact,

$$\hat{U}^\dagger\left(\hat{H} - i\hbar\partial_t\right)\hat{U} = \left(\hat{H} - i\hbar\partial_t\right). \quad (13)$$

The unitary operator (10) is the mechanical counterpart of the Glauber displacement operator, as was pointed out in [5]. Analogous unitary transformations were used frequently in quantum optics, but here we apply this procedure to the motion of classical particles.

The unitary operator $\hat{U}$ has three parts: the first two are just the phase factors. The third one, which plays an essential role in our construction of helical solutions, can also be written as the displacement operator,

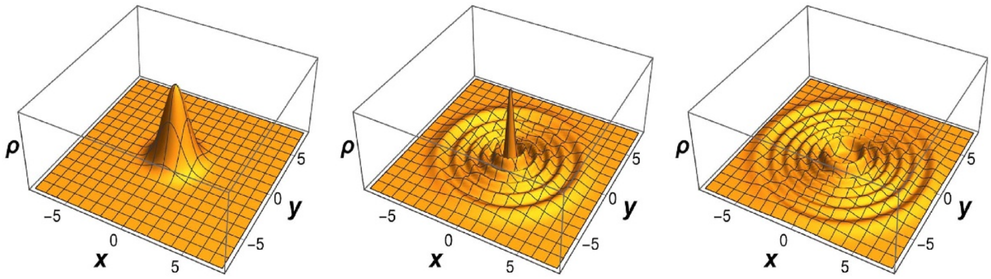

Figure 2. Probability density $\rho = |\psi_{nlp_z}|^2$ as a function of x and y for the following choices of quantum numbers (n,l): (0,0), (5,0) and (5,5).

$$\exp\left[-\frac{i}{\hbar}\hat{p}_i x^i(t)\right] = \exp\left[-x^i(t)\partial_i\right]. \tag{14}$$

When acting on a wave function, it displaces the position variables x^i by $x^i(t)$. To put it more vividly, it injects the classical trajectory $x^i(t)$ into the wave function according to the formula,

$$\exp\left[-x^i(t)\partial_i\right]\psi(x^i) = \psi(x^i - x^i(t)). \tag{15}$$

We will apply now our theorem, to generate families of helical solutions of the Schrödinger equation,

$$i\hbar\partial_t\Phi = -\frac{\hbar^2}{2m}\left[\boldsymbol{\nabla} - \frac{ie}{\hbar}\boldsymbol{A}\right]^2\Phi, \tag{16}$$

from well known (cf for example [6, 7]) stationary solutions ψ_{nlp_z} for a charged particle in the uniform magnetic field,

$$\begin{aligned}\psi_{nlp_z}(x,y,z,t) = \sqrt{\frac{B^{l+1}n!}{2\pi 2^l(n+l)!}}\exp\left[-\frac{i(p_z^2+(2n+1)B\hbar^2)t}{2m\hbar} + \frac{ip_z z}{\hbar} - \frac{B(x^2+y^2)}{4}\right]\\ \times\ (x+iy)^l L_n^l\left[\frac{B(x^2+y^2)}{2}\right],\end{aligned} \tag{17}$$

where L_n^l are associated Laguerre polynomials [8]. The probability density obtained from these solutions depicted in figure 2 does not show any resemblance to the helical trajectories of classical charged particles in figure 1. However, the functions ψ_{nlp_z} can be used as building blocks in the construction of genuine helical solutions. First, note that these solutions depend on z only through the phase factor $\exp(ip_z z/\hbar)$. Therefore, the application of the ICT method to these wave functions would not produce helical trajectories because the probability density will not depend on z. However, we can construct square-integrable wave packets ψ_P from (17) by the integration over p_z with the Gaussian weight $\exp(-d^2p_z^2/(2\hbar^2))$. The resulting wave functions, fully normalized in all three variables and localized on the z axis, have the form,

$$\begin{aligned}\psi_P(x,y,z,t) = \pi^{-1/4}\exp\left[-\frac{mz^2}{2md^2+2i\hbar t}\right]\left(d+\frac{i\hbar t}{md}\right)^{-1/2}\sqrt{\frac{B^{l+1}n!}{2\pi 2^l(n+l)!}}\exp\left[-\frac{i(2n+1)B\hbar t}{2m}\right]\\ \times\exp\left[-\frac{B(x^2+y^2)}{4}\right](x+iy)^l L_n^l\left[\frac{B(x^2+y^2)}{2}\right].\end{aligned} \tag{18}$$

All these wave functions describe wave packets that are held together in the (xy) plane by the magnetic field but they are spreading in time along the z direction. However, only the probability distribution in the ground state (depicted in figure 2) resembles the charge distribution of a classical body. The solutions (18) of the Schrödinger equation will now be used to generate helical solutions.

The application of the ICT method (10) to the wave-packets (18) produces the following wave functions that describe helical trajectories,

$$\psi_H(x,y,z,t) = \hat{U}\psi_P(x,y,z,t) = \pi^{-1/4}e^{-i\delta}\sqrt{\frac{B^{l+1}n!}{2\pi^{3/2}2^l(n+l)!}}\exp\left[-\frac{mz_S^2}{2md^2+2i\hbar t}\right]\left(d+\frac{i\hbar t}{md}\right)^{-1/2} \times \exp\left[-\frac{B(x_S^2+y_S^2)}{4}\right](x_S+iy_S)^l L_n^l\left[\frac{B(x_S^2+y_S^2)}{2}\right], \tag{19}$$

where

$$\delta = \frac{(2n+1)B\hbar t}{2m} + \frac{\boldsymbol{p}(t)\cdot\boldsymbol{r}(t)}{2\hbar} - \frac{\boldsymbol{p}(t)\cdot\boldsymbol{r}}{\hbar}, \tag{20}$$

and we introduced a shortened notation $x_S = x - x(t)$, etc for variables (x,y,z) shifted by the classical solutions. We will not need the explicit form of the phase δ because in what follows we will only discuss the probability density ρ_H,

$$\rho_H(x_S,y_S,z_S,t) = |\psi_H(x,y,z,t)|^2 = N\exp\left[-\frac{m^2d^2z_S^2}{m^2d^4+\hbar^2t^2}\right]\left(d^2+\frac{\hbar^2t^2}{m^2d^2}\right)^{-1/2} \times \exp\left[-\frac{B(x_S^2+y_S^2)}{2}\right](x_S^2+y_S^2)^l L_n^l\left[\frac{B(x_S^2+y_S^2)}{2}\right]^2. \tag{21}$$

The general form of the probability density makes it possible, without doing detailed calculations, to conclude that the center of the wave packet defined as the average value of the position follows exactly the classical trajectory. The average values of x, y and z are obtained by simple shifts of the integration variables in the integrals of the density multiplied by the corresponding coordinate. For example,

$$\begin{aligned}\langle x\rangle &= \int d^3r\, x\rho_H(x-x(t),y-y(t),z-z(t),t)\\ &= \int d^3r\,(x+x(t))\rho_H(x,y,z,t) = x(t).\end{aligned} \tag{22}$$

The integral of $x\rho_H$ vanishes, because after the shift, ρ_H is an even function of x. The same argumentation gives analogous results for the remaining variables,

$$\langle y\rangle = y(t), \quad \langle z\rangle = z(t). \tag{23}$$

Therefore there are no quantum corrections to the motion of the center of the wave packet; it follows exactly the helical classical trajectories shown in figure 1. The name helical solutions of the Schrödinger equation is fully justified. The shape of the wave packet is governed by quantum mechanics. In the present case, the shape of the wave packet in the xy plane does not change in time, but the wave packet spreads in the z direction.

4. Helical solutions of the Dirac equation

The direct application of the ICT method to the Dirac equation is not possible because the Dirac Hamiltonian is not a quadratic expression in positions and momenta. To overcome this problem, we will use the Klein–Gordon equation as an intermediate step in our construction. The connection between the Klein–Gordon equation and the Dirac equation is best seen in the Weyl (chiral) representation [9] of the Dirac matrices. This connection has been employed in [10, 11] to generate new solutions of the Dirac equations in free space.

The Dirac equation in the Weyl representation is a set of two coupled equations for two-dimensional relativistic spinors ϕ and χ,

$$i\lambdabar\left[1/c\,\partial_t+\boldsymbol{\sigma}\cdot\left(\boldsymbol{\nabla}-\frac{ie}{\hbar}\boldsymbol{A}\right)\right]\phi=\chi, \tag{24a}$$

$$i\lambdabar\left[1/c\,\partial_t-\boldsymbol{\sigma}\cdot\left(\boldsymbol{\nabla}-\frac{ie}{\hbar}\boldsymbol{A}\right)\right]\chi=\phi, \tag{24b}$$

where $\lambdabar=\hbar/(mc)$ is the reduced Compton wave length. The electromagnetic potential is chosen in the temporal gauge. The stationary solutions of the Dirac equation in a uniform magnetic field [2] are similar to the corresponding solutions of the Schrödinger equation. They have to be subjected to the same procedure as their nonrelativistic counterparts before they acquire a helical form.

The spinors ϕ and χ that satisfy the Dirac equation have the following property. If the spinor ϕ satisfies the Klein–Gordon equation (with the additional term describing the direct coupling of the magnetic moment to the field),

$$\left[\frac{1}{c^2}\partial_t^2-\left(\boldsymbol{\nabla}-\frac{ie}{\hbar}\boldsymbol{A}\right)^2+\left(\frac{mc}{\hbar}\right)^2-\frac{e}{\hbar}\boldsymbol{\sigma}\cdot\left(\boldsymbol{B}-i\frac{\boldsymbol{E}}{c}\right)\right]\phi=0, \tag{25}$$

then the spinor χ defined by the equation (24a) automatically satisfies the equation (24b). The explicit formulas for the bispinor which satisfies the Dirac equation are (spin up),

$$\Psi_D^u=\begin{bmatrix}\phi\\0\\i\lambdabar(1/c\partial_t+\partial_z-ie/\hbar A_z)\phi\\i\lambdabar(\partial_x-ie\hbar A_x+i\partial_y+e/\hbar A_y)\phi\end{bmatrix}, \tag{26}$$

(spin down),

$$\Psi_D^d=\begin{bmatrix}0\\\phi\\i\lambdabar(\partial_x-ie\hbar A_x-i\partial_y-e/\hbar A_y)\phi\\i\lambdabar(1/c\partial_t-\partial_z+ie/\hbar A_z)\phi\end{bmatrix}. \tag{27}$$

These formulas have been used by us in [10, 11] for the Dirac equation in free space. The construction of the solutions of the Dirac equation from the solutions of the Klein–Gordon equation works also in the presence of the electromagnetic field. In doing so, we reduce the problem of solving the set of two coupled equations (24) to solving just one equation. The use of the solutions of the Klein–Gordon equation as a stepping stone is particularly well suited in the present case, because this equation is of the second order in space derivatives and the ICT method can be applied.

To obtain helical solutions of the Dirac equation, we proceed in several steps. First, we transform the Klein–Gordon equation for spin up to the form,

$$\left[\frac{4}{c^2}\partial_+\partial_--(\partial_x+iBy/2)^2-(\partial_y-iBx/2)^2+\left(\frac{mc}{\hbar}\right)^2-B\right]\Psi_{KG}^u=0, \tag{28}$$

where

$$t_{\pm} = t \pm z/c \text{ and } \partial_{\pm} = \partial/\partial t_{\pm} = \frac{1}{2}(\partial_t \pm c\partial_z). \tag{29}$$

In order to obtain helical solutions by the ITC method, we convert the equation (28) into the Schrödinger-like form. This can be done for a restricted class of functions Ψ^u_{KG}, with a special form of the time dependence, namely for those functions whose time dependence on t_+ is harmonic with the frequency $\omega = Mc^2/\hbar$. We also extract from Ψ^u_{KG} an additional factor harmonic in t_-,

$$\Psi^u_{KG} = \exp\left[-\frac{i\left(M^2c^2t_+ + m^2c^2t_- - \hbar^2 Bt_-\right)}{2M\hbar}\right]\Phi. \tag{30}$$

The equation satisfied by Φ has the form of the Schrödinger equation in two spatial dimensions with t_- playing the role of time,

$$i\hbar\partial_-\Phi = -\frac{\hbar^2}{2M}\left[\partial_x^2 + \partial_y^2 - \frac{B^2(x^2+y^2)}{4} - iB(x\partial_y - y\partial_x)\right]\Phi. \tag{31}$$

Now we have at our disposal all stationary solutions (17) of the Schrödinger equation. The only difference is a change in notation: p_z is put equal to 0, t is replaced by t_-, and m is replaced by M. Our ICT theorem can now be applied to generate the solutions with injected classical trajectories $x(t_-)$ and $y(t_-)$ defined by (8). The resulting wave function Ψ^{nl}_{KG} satisfying the Klein–Gordon equation is,

$$\Psi^{nl}_{KG} = e^{-i\varphi}C^l_n L^l_n\left[B/2(x_S^2+y_S^2)\right], \tag{32}$$

where

$$\varphi = \frac{M^2c^2t_+ + \left(m^2c^2 + 2n\hbar^2 B\right)t_-}{2M\hbar} + \frac{1}{2\hbar}\left(x(t_-)p_x(t_-) + y(t_-)p_y(t_-)\right) - \frac{1}{\hbar}\left(xp_x(t_-) + yp_y(t_-)\right), \tag{33}$$

$$C^l_n = \exp\left[-B/4(x_S^2+y_S^2)\right](x_S + iy_S)^l. \tag{34}$$

We may visualize these wave functions by going back to figure 2 and applying the following transformations. First, we shift the shapes depicted there away from the center. Next, we start rotating them around the center with the cyclotron frequency. Finally, we move this structure with the speed of light along the z axis to create a helix.

We started our construction of the function Ψ^{nl}_{KG} with the solutions of the Klein–Gordon equation in the form (30). This construction guarantees that Ψ^{nl}_{KG} contains only the positive energy parts, as required to describe electrons with no parts describing positrons. However, the ICT method injects classical trajectories which clearly introduce time dependence with both signs of the frequency due to the presence of trigonometric functions. It may seem that this might introduce parts describing antiparticles. We checked that in the function Ψ^{nl}_{KG} all terms with the opposite sign cancel out. It must be so on physical grounds; the homogeneous magnetic field cannot supply the energy.

The requirement of positive energy is often ignored. For example, the solution of the Dirac equation in the presence of a plane electromagnetic wave (Wolkow wave function [12]) contains terms with both signs of the frequency. Therefore, it does not describe the state of an electron but it has a significant positron component [13].

Our solution of the Klein–Gordon equation Ψ^{nl}_{KG} depends on 5 arbitrary parameters (in addition to two quantum numbers n and l): on M and on the initial values of the injected trajectory (8). Therefore, Ψ^{nl}_{KG} may serve as the generating function for the plethora of various solutions because all linear operations on the wave function (for example, differentiation or integration with respect to the parameters) will produce different solutions. From all these solutions of the Klein–Gordon equation we can generate the solutions of the Dirac equation using the formulas (26) and (27).

Since the function Ψ_{KG}^{nl} depends on a free parameter M we could construct the wave packets analogous to those for the Schrödinger equation (18) by integrating over M with some weight function. However, such wave packets are not interesting because the integration over M obfuscates the helical form of the solutions. The reason for this is that M defines the cyclotron frequency and the integration over frequencies blurs the helical motion. In the nonrelativistic theory the construction of helical wave packets is possible because in this approximation the cyclotron frequency is fixed; it does not depend on the energy.

In the last step of the construction of the helical Dirac wave function, we generate the bispinor Ψ_D according to the formula (26),

$$\Psi_D^{nl} = \frac{1}{\sqrt{N}} e^{-i\varphi} C_n^l \begin{bmatrix} L_n^l \\ 0 \\ \frac{M}{m} L_n^l \\ c_1 L_n^l + c_2 L_{n-1}^{l+1} \end{bmatrix}, \tag{35}$$

where

$$N = \frac{2^{l-1}\pi(n+l)!}{n! m^2 c^2 B^{l+1}} \left[4(m^2+M^2)c^2 + 8nB\hbar^2 + (B\hbar x(t_-) - 2p_y(t_-))^2 + (B\hbar y(t_-) + 2p_x(t_-))^2\right], \tag{36}$$

$$c_1 = -\frac{1}{2mc}\left[B\hbar y(t_-) + 2p_x - i(B\hbar x(t_-) - 2p_y(t_-))\right], \quad c_2 = -\frac{i}{mc}\left[B\hbar(x_S + iy_S)\right]. \tag{37}$$

To condense the notation we omitted the argument $B(x_S^2 + y_S^2)/2$ of the Laguerre polynomials. Note that the bispinor Ψ_D^{nl} is normalized only in the transverse direction. Its dependence on z is periodic. The probability density associated with the Dirac bispinor (35) is,

$$\rho_D^{nl} = \frac{1}{Nm^2c^2} \exp\left[-B/2(x_S^2+y_S^2)\right](x_S^2+y_S^2)^l \left[d_1 (L_n^l)^2 + d_2 (L_{n-1}^{l+1})^2 + d_3 L_n^l L_{n-1}^{l+1}\right], \tag{38}$$

where

$$\begin{aligned} d_1 &= \frac{1}{m^2c^2}\left[(m^2+M^2)c^2 + (B\hbar x(t_-) - 2p_y(t_-))^2/4 + (B\hbar y(t_-) + 2p_x(t_-))^2/4\right], \\ d_2 &= \frac{B^2\hbar^2}{m^2c^2}\left[x_S^2 + y_S^2\right], \qquad d_3 = -\frac{B\hbar}{m^2c^2}\left[x_S(B\hbar x(t_-) - 2p_y(t_-)) + y_S(B\hbar y(t_-) + 2p_x(t_-))\right]. \end{aligned} \tag{39}$$

With the use of the probability density ρ_D^{nl} we generate the helical curves (shown in figure 3) which provide a link with classical trajectories (shown in figure 1). These curves are obtained as follows. For a fixed value of t we calculate the average values $\langle x\rangle$ and $\langle y\rangle$ as functions of z,

$$\begin{aligned} \langle x\rangle_t(z) &= \int dxdy\, x\rho(x,y,t-z/c), \\ \langle y\rangle_t(z) &= \int dxdy\, y\rho(x,y,t-z/c). \end{aligned} \tag{40}$$

In figure 3 we show the plots of $(\langle x\rangle_t(z), \langle y\rangle_t(z), z)$.

In all cases, except when $n = 0 = l$, the last term in (38) is different from zero. Since d_3 contains terms linear in x_S and y_S, the average values $\langle x_S\rangle$ and $\langle y_S\rangle$ do not vanish. This produces corrections to the classical orbit. The total average values $\langle x\rangle$ and $\langle y\rangle$ are the sums of classical trajectories and corrections, These corrections do not depend on l and their dependence on n is shown in the following formulas,

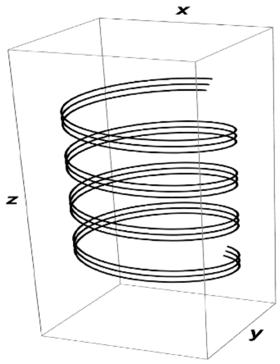

Figure 3. Three helical lines obtained as parametric plots of $(\langle x\rangle_t(z), \langle y\rangle_t(z), z)$ for the three consecutive values of time.

$$\langle x\rangle = x(t) + \frac{4n\hbar(\hbar Bx(t_-) - 2p_y(t_-))}{4(m^2+M^2)c^2 + 8n\hbar^2 B + (\hbar Bx(t_-) - 2p_y(t_-))^2 + (\hbar By(t_-) + 2p_x(t_-))^2}, \quad (41a)$$

$$\langle y\rangle = y(t) + \frac{4n\hbar(\hbar By(t_-) + 2p_x(t_-))}{(m^2+M^2)c^2 + 8n\hbar^2 B + (\hbar Bx(t_-) - 2p_y(t_-))^2 + (\hbar By(t_-) + 2p_x(t_-))^2}. \quad (41b)$$

In the nonrelativistic limit ($c\to\infty$) and also in the classical limit ($\hbar\to 0$) the corrections vanish and we obtain the classical trajectories, as is the case of the Schrödinger equation.

The corrections (41) to the classical helical orbits are minuscule. The largest value of these corrections is about $4n\times 10^{-13}$ m. Therefore, the distortion of classical orbits is completely negligible.

5. Conclusions

The results presented in this work serve a dual purpose. On the one hand, they add new analytic solutions of the Schrödinger and Dirac equations that have a clear physical relevance. On the other hand they may be viewed as explicit examples of the validity of the Ehrenfest theorem [14, 15] in relativistic quantum mechanics. In this context we found significant differences between the non-relativistic and relativistic theories. Despite their similarities, these two cases are substantially different. In the non-relativistic case we were able to construct electron wave packets localized in all three dimensions moving along classical trajectories, in accordance with the Ehrenfest theorem. In the relativistic case the wave packets were localized only in the transverse direction. Therefore, they describe a trajectory of electrons extending over all values of z.

Data availability statement

All data that support the findings of this study are included within the article (and any supplementary files).

Acknowledgments

We thank the Referee for a very thorough and useful report that resulted in many corrections and clarifications.

Appendix

The first factor of the unitary operator $\hat{U}$ is a c-number phase factor; it has no effect on the Hamiltonian operator but it affects the time derivative. The second factor leaves the position operators unchanged but shifts the momentum operator by the classical solution and the third factor has the analogous effect on the position operator,

$$\exp\left[-\frac{i}{\hbar}p_i(t)\hat{x}^i\right]\hat{p}_i\exp\left[\frac{i}{\hbar}p_i(t)\hat{x}^i\right] = \hat{p}_i + p_i(t), \tag{A.1}$$

$$\exp\left[\frac{i}{\hbar}\hat{p}_i x^i(t)\right]\hat{x}^i\exp\left[-\frac{i}{\hbar}\hat{p}_i x^i(t)\right] = \hat{x}^i + x^i(t). \tag{A.2}$$

Therefore, the action of the operator $\hat{U}$ on the Hamiltonian operator gives,

$$\hat{U}^\dagger\hat{H}\hat{U} = \frac{1}{2}(\hat{p}_i + p_i(t))A^{ij}(\hat{p}_i + p_i(t)) + \frac{1}{2}(\hat{x}^i + x^i(t))B_{ij}(\hat{x}^j + x^j(t)) + (\hat{p}_i + p_i(t))C^i{}_j(\hat{x}^j + x^j(t)). \tag{A.3}$$

The transformation of the time derivative gives,

$$\hat{U}^\dagger i\hbar\partial_t\hat{U} = i\hbar\partial_t + \frac{1}{2}\left(p_i(t)\frac{dx^i(t)}{dt} - \frac{dp_i(t)}{dt}x^i(t)\right) - \frac{dp_i(t)}{dt}\hat{x}^i + \frac{dx^i(t)}{dt}\hat{p}^i. \tag{A.4}$$

In the last step we use the equations of motion (11). One may check now that all terms quadratic and linear in $x^i(t)$ and $p_i(t)$ cancel out in the difference between (A.3) and (A.4). Therefore, the equality,

$$\hat{U}^\dagger(\hat{H} - i\hbar\partial_t)\hat{U} = \hat{H} - i\hbar\partial_t. \tag{A.5}$$

is valid.

ORCID iD

Iwo Bialynicki-Birula https://orcid.org/0000-0002-5195-4133

References

[1] Fock V 1928 Bemerkung zur Quantelung des harmonischen Oszillators im Magnetfeld *Z. Phys.* **47** 446
[2] Rabi I I 1928 Das freie Elektron im homogenen Magnetfeld nach der Diracschen Theorie *Z. Phys.* **49** 507
[3] Bagrov V G and Gitman D M 1990 *Exact Solutions of Relativistic Wave Equations* (Dordrecht: Kluver)
[4] García-Ripoll J J, Pérez-García V M and Vekslerchik V 2001 Construction of exact solutions by spatial translations in inhomogeneous nonlinear Schrödinger equations *Phys. Rev.* E **64** 056602
[5] Bialynicki-Birula I and Bialynicka-Birula Z 2002 Center-of-mass motion in the many-body theory of Bose-Einstein condensates *Phys. Rev.* A **65** 063606
[6] Ballentine L E 1990 *Quantum Mechanics* (Singapore: World Scientific) p 314
[7] Bialynicki-Birula I, Cieplak M and Kaminski J 1992 *Theory of Quanta* (Oxford: Oxford University Press) p 237

[8] Wolfram Research, Inc. 2022 *Mathematica, Version 13.2* (Champaign, IL: Wolfram Research, Inc.)
[9] Weyl H 1931 *The Theory of Groups and Quantum Mechanics* (New York: Dover) p 213
[10] Bialynicki-Birula I and Bialynicka-Birula Z 2017 Relativistic electron wave packets carrying angular momentum *Phys. Rev. Lett.* **118** 114801
[11] Bialynicki-Birula I and Bialynicka-Birula Z 2019 Twisted localized solutions of the Dirac equation: Hopfionlike states of relativistic electrons *Phys. Rev.* A **100** 012108
[12] Wolkow D M 1935 Über eine Klasse von Lösungen der Diracschen Gleichung *Z. Phys.* **94** 250
[13] Bialynicki-Birula I and Bialynicka-Birula Z 2020 Comment on "Nondispersive analytical solutions to the Dirac equation" *Phys. Rev. Res.* **2** 038001
[14] Ehrenfest P 1927 Bemerkung uber die angenäherte Gültigkeit der klassischen Mechanik innerhalb der Quantenmechanik *Z. Phys.* **45** 455
[15] Bialynicki-Birula I and Bialynicka-Birula Z 2022 Ehrenfest theorem in relativistic quantum theory *J. Phys. B: At. Mol. Opt. Phys.* **55** 114001